Available online at www.sciencedirect.com

SciVerse ScienceDirect

Journal of the European Ceramic Society 32 (2012) 1971–1976

www.elsevier.com/locate/jeurceramsoc

Synthesis and characterization of nanometric yttrium-doped hafnia solid solutions

B. Matović [a], D. Bučevac [a,*], M. Prekajski [a], V. Maksimović [a], D. Gautam [b], K. Yoshida [c], T. Yano [c]

[a] *Institute of Nuclear Sciences Vinca, Belgrade University, 11001 Belgrade, Serbia*

[b] *Nanoparticle Process Technology, Department of Engineering Sciences, University of Duisburg-Essen, Lotharstrasse 1, MA 343, D-47057, Duisburg, Germany*

[c] *Tokyo Institute of Technology, Research Laboratory for Nuclear Reactors, 2-12-1, O-okayama, Meguro-ku, Tokyo 152-8550, Japan*

Available online 9 November 2011

Abstract

Nanometric-sized yttrium doped HfO_2 powders were obtained by applying metathesis and combustion reactions. The tailored composition of solid solutions was: $Hf_{1-x}Y_xO_{2-\delta}$ with concentration "x" ranging from 0 to 0.2. $HfCl_4$ was used as a source of hafnium whereas $Y(NO_3)_3{\cdot}6H_2O$ was used as a source of yttrium. The obtained powders were annealed at different temperatures in order to induce crystallization of HfO_2. The influence of dopant concentration, annealing temperature and annealing time on powder properties was examined. The XRD analysis revealed that the crystal structure of HfO_2 depends on the dopant concentration. The samples doped with 20 mol% of yttrium and annealed at 1500 °C had high-temperature, cubic structure even after cooling to room temperature. The presence of relatively large amount of dopant was beneficial in stabilizing highly desirable cubic phase of HfO_2. It was found that the crystallite size lies in the nanometric range (<10 nm).

Keywords: A. Calcination; B. X-ray methods; C. Chemical properties; E. Insulators; HfO_2

1. Introduction

Hafnium dioxide (HfO_2), known as hafnia, is technologically important ceramic material with good physicochemical characteristics such as large bandgap (5.5–6 eV), relatively high dielectric constant (22–25), high breakdown field (3.9–6.7 MV/cm), high thermal stability, large heat of formation (−271 kcal/mol) and high neutron absorption coefficient.[1–5] It is used in many fields like high K gate dielectric,[6,7] oxygen sensor,[8] electrolyte for solid oxide fuel cells (SOFC),[9] scintillator and X-ray phosphor.[10,11] Physical and chemical properties of hafnia are very similar to those of zirconia (ZrO_2).[12] The both compounds have a high melting point; zirconia 2690 °C and hafnia 2900 °C, which makes them very useful as high temperature refractory materials.[13] Similar to zirconia, pure HfO_2 has a monoclinic crystal structure at room temperature which transforms to tetragonal and cubic structure at elevated temperatures.[14] The volume expansion caused by the tetragonal to monoclinic transformation induces large stresses which normally cause cracking of pure HfO_2 upon cooling from high temperature. Several studies have reported that the addition of oxides such as MgO, Y_2O_3 and CaO is an effective way to stabilize the tetragonal and/or cubic phase.[15,16] The cubic phase of hafnia has a very low thermal conductivity which has led to its use as a thermal barrier coating in jet and diesel engines. The low thermal conductivity allows operation of these engines at much higher temperature.[17] Thermodynamically speaking, the higher the operation temperature of an engine, the greater the efficiency. It is also expected that hafnia can be useful as coating material to improve oxidation resistance of spacecraft during its reentry into the Earth's atmosphere.[18]

It is well known that the sintering temperature decreases when nanosized powders are used. Therefore it is important to obtain powders of high quality with particle size in the nanometric range. The metathesis synthesis (MS)[19] and combustion glycine nitrate process (GNP)[20] are promising methods to produce a single phase, highly pure nanosized powders with a precise stoichiometry. According to the literature data, hafnia and its solid solutions have not been obtained by these two methods so far.

2. Materials and methods

Starting chemicals used for the synthesis were hafnium chloride ($HfCl_4$), yttrium nitrate hexahydrate ($Y(NO_3)_3{\cdot}6H_2O$),

* Corresponding author. Tel.: +381 11 3408723; fax: +381 11 3408723.
E-mail address: bucevac@vinca.rs (D. Bučevac).

0955-2219/$ – see front matter © 2011 Elsevier Ltd. All rights reserved.
doi:10.1016/j.jeurceramsoc.2011.10.029

sodium hydroxide (NaOH) and glycine ($C_2H_5NO_2$) from Alfa Aesar, Germany. The compositions of the starting reacting mixtures were calculated according to the nominal composition of the final reaction products. The following compositions with varying mole fraction of yttrium were prepared and the samples were coded as HfY*X*, where $X = 5$, 10, 15 and 20 mol%.

2.1. Metathesis synthesis (MS)

MS procedure is based on the process involving the exchange of bonds between metal chlorides ($HfCl_4$) and/or metal nitrates ($Y(NO_3)_3{\cdot}6H_2O$) with sodium hydroxide (NaOH), which results in a creation of products with similar or identical bonding affiliations. The reaction of ion exchange takes place in a solid state. The reaction can be described by the following equation where δ refers to the formation of oxygen vacancies due to maintaining an electrical neutrality of crystal lattice:

$$2[(1-x)HfCl_4 + xY(NO_3)_3{\cdot}6H_2O] + 2(4-x)NaOH + (x/2-\delta)O_2 \rightarrow 2Hf_{1-x}Y_xO_{2-\delta} + 8(1-x)NaCl + 6xNaNO_3 + (11x+4)H_2O \quad (1)$$

The calculated amounts of chemicals were hand mixed in an alumina mortar with an alumina pestle for about 5 min. The mixture of reaction products was rinsed in a centrifuge-Megafuge 1.0, Heraeus, at 3500 rpm to remove NaCl and $NaNO_3$. Each washing run was performed for 10 min. This procedure was repeated three times with distilled water and twice with ethanol.

2.2. Glycine nitrate process (GNP)

The other applied method for hafnia synthesis was glycine nitrate process. This procedure is based on the exothermicity of the redox reaction between the fuel (glycine) and oxidizer (nitrite and chlorite). The procedure needs to be performed in three stages. The first one is dissolution of metal chloride, metal nitrite and glycine in water. The second stage is autoignition of solution at about 180 °C which is followed by the self-sustaining combustion giving ash as a product. Finally, the third stage is annealing of ash. The role of annealing is to burn out the organic components and obtain pure oxide powder. The synthesis reaction for hafnia could be described by the following equation:

$$HfCl_4 + 4C_2H_5NO_2 + 10O_2 \rightarrow HfO_2 + 10H_2O + 2N_2 + 8CO_2 + 2Cl_2 \quad (2)$$

2.3. Characterization

The obtained powders were analyzed by X-ray diffraction (XRD), thermogravimetric analysis (TGA) and differential thermal analysis (DTA). The powders were subsequently annealed at temperature ranging from 600 to 1500 °C in order to examine the effect of annealing temperature on the crystallization process. The annealing was performed in air, under atmospheric pressure. The samples obtained by GNP method were held at annealing temperature from 30 to 240 min to analyze the effect of annealing time on crystallite size. The crystallite size was determined from XRD patterns collected using a Simens X-ray Diffractometer (Kristaloflex 500) with Ni filtered Cu K_α radiation ($\lambda = 0.1541$ nm). The measurements were performed in the range 10–80° 2θ in a continuous scan mode with a step width of 0.02° and at a scan rate of 1° 2θ/min. Before the measurement the angular correction was done by quality Si standard. The obtained data were fitted using peak-fitting program.[21] The Lorentizian function gave the best fit to the experimental data. Scanning electron microscopy (FE-SEM field-emission type, S-4800, Hitachi, Japan) was used to study the morphology of obtained powders.

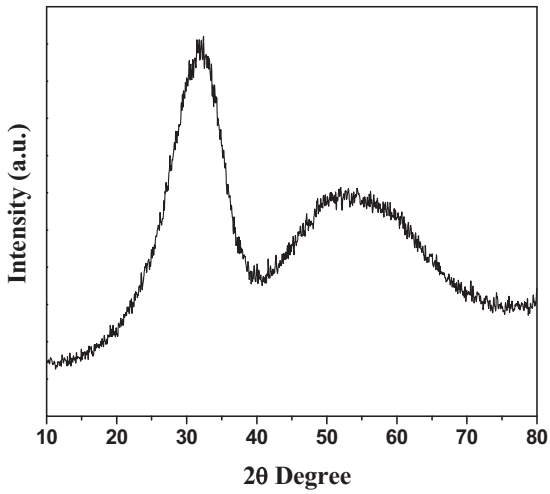

Fig. 1. XRD pattern of as-prepared, undoped, HfY0 powder obtained by metathesis synthesis.

3. Results and discussion

Undoped hafnia (HfY0) was analyzed first. Typical X-ray diffraction pattern of the as-prepared sample obtained by the metathesis synthesis reaction is shown in Fig. 1. The presence of two broad peaks reveals that the sample is amorphous. This indicates that the double displacement reaction (Eq. (1)) does not lead to formation of crystalline phase at room temperature.

In order to better understand the mechanism of metathesis synthesis the reaction products were studied by thermal analysis. It is well known that $HfCl_4$ reacts spontaneously with liquid water and water vapor to produce an oxychloride octahydrate ($HfOCl_2{\cdot}8H_2O$) or hydrated oxychloride ($HfOCl_2{\cdot}H_2O$).[22] Thus, $HfCl_4$ can be in different hydration state and the synthesis is more complex than the reaction mentioned before (Eq. (1)). Thermal analysis of undoped, as-prepared, HfY0 powder shows that DTA and TGA curves are characterized by two peaks. The first one is an endothermic peak between 50 and 100 °C due to dehydration. The second one is very broad, exothermic peak at about 300 °C due to crystallization of the amorphous material (Fig. 2). The endothermic effect is accompanied by the mass loss due to the evaporation of absorbed water. The mass loss terminates at 300 °C, at which point the crystalline water is lost. It is also known that the weight loss at 300 °C could be attributed to the sublimation of unreacted $HfCl_4$.[23] In order to intensify crystallization of as-prepared HfY0 the powders were annealed at

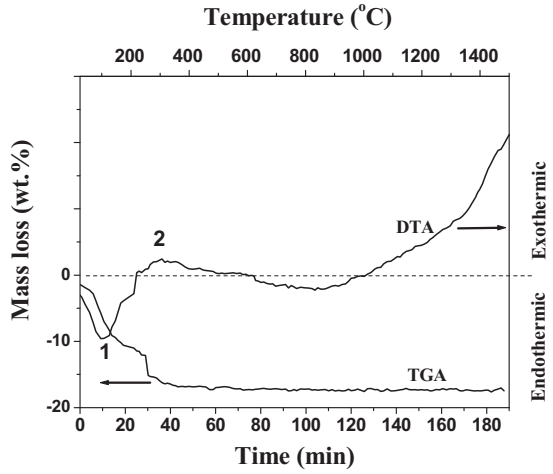

Fig. 2. DTA and TGA traces of undoped, as-prepared, HfY0 powder obtained by metathesis synthesis.

600 °C and 1500 °C. XRD of sample annealed at 600 °C (Fig. 3) exhibits fairly broad peaks, which could be indexed as HfO_2 with monoclinic $P2_1/c$ structure.[24] As Fig. 4 shows, the further increase in annealing temperature to 1500 °C narrows the XRD peaks which indicates almost complete crystallization of HfO_2.

Fig. 5 shows the SEM image of undoped HfY0 powder annealed at 600 °C. The high magnification image reveals that the hafnia sample consists of many domains with relatively uniform size (∼5 nm) which are aggregated into snowflake-like structures.

Based on the above results it can be concluded that annealing temperature of 1500 °C is sufficiently high to obtain well-crystallized undoped HfO_2 powder. Now it would be of great value to analyze the XRD patterns of HfO_2 powders with different dopant concentrations annealed at 1500 °C (Fig. 6). Diffraction peaks corresponding to either yttrium oxide or hydroxide were not observed indicating the formation of solid solution in the entire composition range. Furthermore, the XRD patterns reveal that the different additive concentrations result in different crystal structure of hafnia. The XRD pattern of

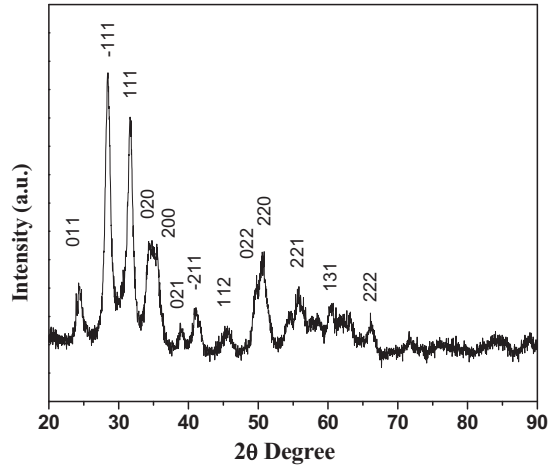

Fig. 3. Room temperature XRD pattern of undoped HfY0 powder obtained by metathesis synthesis annealed at 600 °C for 5 min.

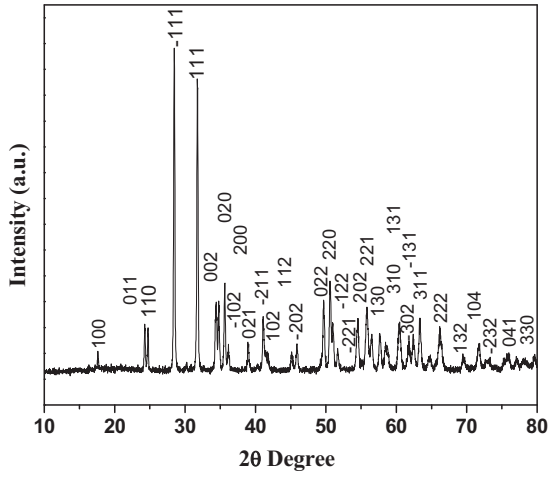

Fig. 4. Room temperature XRD pattern of undoped HfY0 powder obtained by metathesis synthesis annealed at 1500 °C for 5 min.

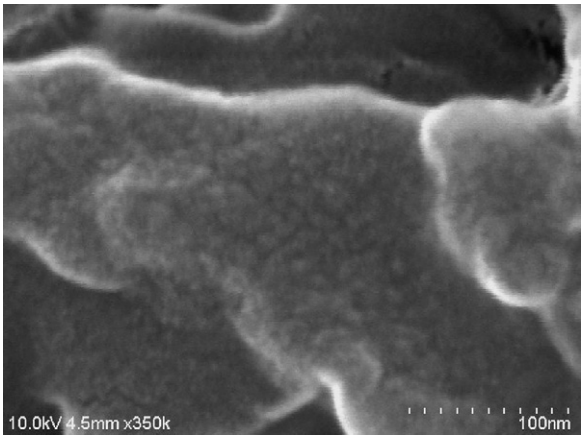

Fig. 5. FE-SEM image of undoped HfY0 powder obtained by metathesis synthesis annealed at 600 °C for 5 min.

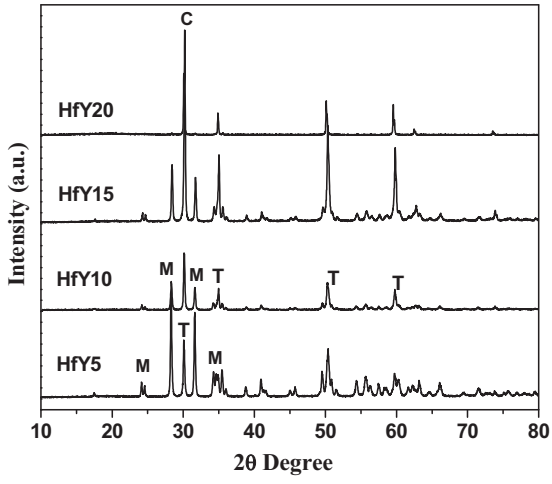

Fig. 6. Room temperature XRD patterns of HfO_2 doped with 5, 10, 15 and 20 mol% of yttrium annealed at 1500 °C for 5 min. M, monoclinic; T, tetragonal; and C, cubic.

Table 1
XRD characteristics of solid solutions obtained by the metathesis synthesis annealed at 1500 °C for 5 min.

Composition	Monoclinic (%)	Tetragonal (%)	Cubic (%)
HfY5	82.1	17.9	–
HfY10	53.7	46.3	–
HfY15	41.2	58.8	–
HfY20	–	–	100

sample with 5 mol% of dopant reveals that the main phase is monoclinic polymorph of HfO_2 which is stable at room temperature. High temperature polymorph, tetragonal HfO_2, is identified as a secondary phase. It is worth noting that the tetragonal HfO_2 was not detected in undoped HfO_2 (Fig. 4). The intensity of monoclinic reflections decreases with yttrium concentration and finally the monoclinic reflections disappear in composition with 20 mol% of yttrium which has only cubic structure. The yttrium dopant concentration of 20 mol% is sufficient to stabilize high-temperature, cubic, polymorph of HfO_2 which does not transform to the monoclinic polymorph during cooling to room temperature.

The explanation of this behavior was found in the fact that predominantly covalent nature of Hf–O bond favors the sevenfold coordination (7 CN) of Hf^{4+} cation in monoclinic polymorph. On the other side, the ideal ionic size ratio of MO_8 eight-coordination oxide such as cubic and tetragonal polymorphs is 0.732. Since hafnia possesses the fluorite (cubic) structure with lower $r(Hf^{4+})/r(O^{2-})$ ratio (0.703), the transformation to monoclinic polymorph is expected. However, it is possible to obtain hafnia with cubic and tetragonal structure at room temperature by doping with aliovalent cations such as Y^{3+}, which possess a lower valence and larger ionic size than Hf^{4+}. According to Shannon's compilation,[25] the ionic radii of Hf^{4+} and Y^{3+} for CN 8, are 0.97 and 1.053 Å, respectively. Thus, the increase in dopant amount in hafnia crystal structure leads to stabilization of cubic structure. In addition, the incorporation of Y^{3+} cations is accompanied by formation of oxygen vacancies due to maintaining an electrical neutrality of crystal lattice. The formation of oxygen vacancies has also influence on complete stabilization of the cubic phase.[26]

The volume fraction of different hafnia polymorphs was estimated from the integrated intensities of the diffraction lines following the procedure proposed by Toraya et al.[27] (Table 1). The chosen diffraction lines were −111 and 111 for monoclinic hafnia and 101 for tetragonal hafnia.

Since, the fluorite-type solid solution with cubic lattice was retained to room temperature in the presence of 20 mol% yttrium only samples with this dopant concentration were prepared by the combustion synthesis. During GNP synthesis (Eq. (2)), a large amount of volatile products escapes from the system resulting in highly porous material (Fig. 7).

DTA analysis of the powder obtained by GNP shows three exothermic peaks at 220, 320 and 580 °C (Fig. 8). It is believed that the first two peaks are the result of decomposition of organic residue which is present in the ash obtained after combustion. This finding is also supported by the TGA analysis which shows

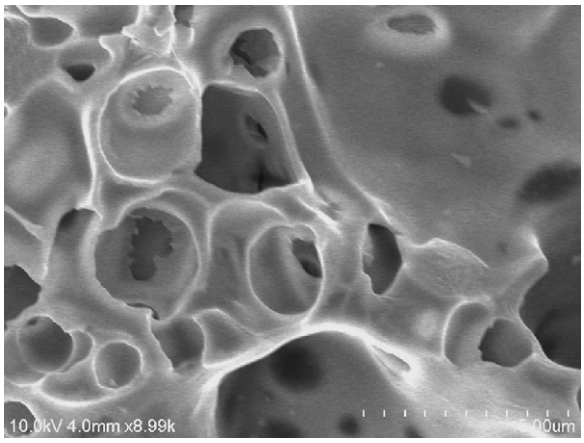

Fig. 7. SEM image of HfY20 powder obtained by GNP method.

that the considerable weight loss is measured at temperatures below 500 °C. Since the main goal of this study was to analyze the obtained hafnia powder the detailed results on decomposition of the precursors will be presented in future publication.

The third peak (580 °C) is the result of the crystallization of amorphous phase. In order to better understand the crystallization process, the XRD patterns of the samples annealed at the above mentioned temperatures were presented in Fig. 9. As can be seen, the samples annealed at 220 and 320 °C are mainly amorphous indicating that these temperatures are not high enough to cause crystallization. However, the powder annealed at 580 °C is well crystallized with sharp peaks related to fluorite, cubic, structure. This indicates that 20 mol% Y doped hafnia directly crystallizes into the cubic structure.

In order to study the effect of annealing temperature as well as the effect of annealing time on crystallite size, the as-prepared powders were annealed at 600 and 800 °C for different times. The crystallite size was calculated from XRD data (Fig. 10) using Scherrer's method.[28] The results of change of crystallite size with annealing temperature and holding time are given in Table 2. It was found that the crystallite size slightly increases as the annealing temperature increases from 600 °C to 800 °C.

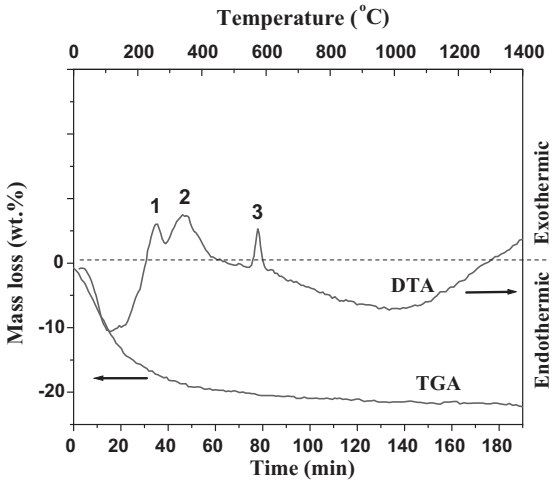

Fig. 8. DTA and TGA traces of HfY20 sample obtained by GNP method.

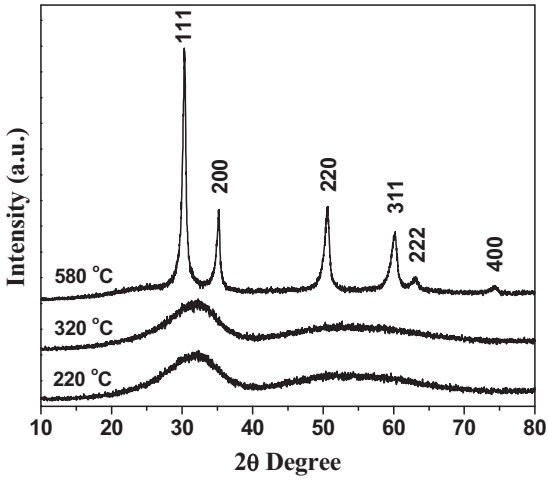

Fig. 9. Room temperature XRD patterns of HfY20 powder obtained by GNP annealed at different temperatures according DTA maximums.

The average crystallite size of these samples is measured to be less than 10 nm even after annealing for 240 min. However, an increase in annealing temperature to 1000 °C causes a considerable increase in crystallite size.

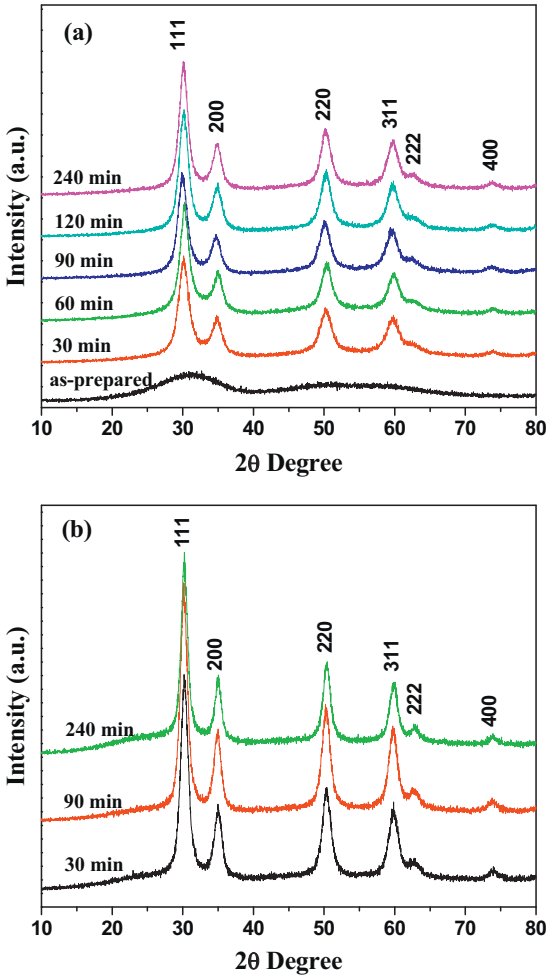

Fig. 10. Room temperature XRD patterns of HfY20 obtained by GNP annealed at (a) 600 °C and (b) 800 °C for different soaking time.

Table 2
Crystallite size (nm) as a function of annealing temperature and holding time for samples obtained by GNP.

Temperature (°C)	Time (min)				
	30	60	90	120	240
600	4.6	4.9	5.2	5.4	5.8
800	7.2		7.7		8.6
1000	16.8		28.5	34.0	

4. Conclusions

Yttrium doped hafnia solid solutions ($Hf_{1-x}Y_xO_{2-\delta}$) with "x" ranging from 0 to 0.2 were prepared by applying metathesis and combustion reactions. Five minutes long annealing of as-prepared, amorphous, powders at 1500 °C caused complete crystallization of hafnia solid solutions. XRD patterns revealed that the different dopant concentrations result in different crystal structures of hafnia. The presence of 15 mol% of yttrium dopant was not sufficient to stabilize high-temperature, cubic polymorph of HfO_2 after annealing at 1500 °C. However, the sample doped with 20 mol% of yttrium directly crystallized in a cubic structure which stayed stable after cooling to room temperature. It was found that the crystallite size of samples annealed at temperature below 1000 °C lies in the nanometric range (<10 nm).

Acknowledgments

This project was financially supported by the Ministry of Education and Science of Serbia (project number: 45012). One of the authors (Branko Matovic) gratefully acknowledges the financial support from the Tokyo Institute of Technology, Research Laboratory for Nuclear Reactors, 2-12-1, O-okayama, Meguro-ku, Tokyo 152-8550, as a visiting professor.

References

1. Nahar RK, Singh V, Sharma A. Study of electrical and microstructure properties of high dielectric hafnium oxide thin film for MOS devices. *J Mater Sci Electron* 2007;**18**:615–9.
2. Wilk GD, Wallace RM, Anthony JM. Hafnium and zirconium silicates for advanced gate dielectrics. *J Appl Phys* 2000;**87**:484–92.
3. Hubbard KJ, Schlom DG. Thermodynamic stability of binary oxides in contact with silicon. *J Mater Res* 1996;**11**:2757–76.
4. McPherson J, Kim JY, Shanware A, Mogul H. Thermochemical description of dielectric breakdown in high dielectric constant materials. *Appl Phys Lett* 2003;**82**:2121–3.
5. Valdez JA, Usov IO, Won J, Tang M, Dickerson RM, Jarvinen GD, et al. 10 MeV Au ion irradiation effects in an MgO–HfO_2 ceramic–ceramic (CERCER) composite. *J Nucl Mater* 2009;**393**:126–33.
6. Filipescu M, Scarisoreanu N, Craciun V, Mitu B, Purice A, Moldovan A, et al. High-k dielectric oxides obtained by PLD as solution for gates dielectric in MOS devices. *Appl Surf Sci* 2007;**253**:8184–91.
7. Demkov AA, Sharia O, Luo X, Bersuker G, Robertson J. Modeling complexity of a complex gate oxide. *Microelectron Eng* 2009;**86**:1763–6.
8. Izu N, Itoh T, Shin W, Matsubara I, Murayama N. The effect of hafnia doping on the resistance of ceria for use in resistive oxygen sensors. *Sens Actuators B* 2007;**123**:407–12.

9. Trubelja MF, Stubican VS. Ionic conductivity in the hafnia–R_2O_3 systems. *Solid State Ionics* 1991;**49**:89–97.
10. Kirm M, Aarik J, Jurgens M, Sildos I. Thin films of HfO_2 and ZrO_2 as potential scintillators. *Nucl Instrum Methods Phys Res Sect A* 2005;**537**:251–5.
11. LeLuyer C, Villanueva-Ibanez M, Pillonnet A, Dujardin C. HfO_2:X (X = Eu, Ce, Y) sol gel powders for ultradense scintillating materials. *J Phys Chem A* 2008;**122**:10152–5.
12. Yashima M, Takahashi H, Ohtake K, Hirose T, Kakihana M, Arashi H, et al. Formation of metastable forms by quenching of the HfO_2–$RO_{1,5}$ melts (R = Gd, Y and Yb). *J Phys Chem Solids* 1996;**57**:289–95.
13. Glushkova VB, Kravchinskaya MV. HfO_2-based refractory compounds and solid solutions. *Ceram Int* 1985;**11**:56–65.
14. Lynch CT. *High temperature oxides*. New York: Academic Press; 1970.
15. Andrievskaya ER. Phase equilibria in the refractory oxide systems of zirconia hafnia and yttria with rare-earth oxides. *J Eur Ceram Soc* 2008;**28**:2363–88.
16. Mann M, Kolis J. Hydrothermal crystal growth of yttrium and rare earth stabilized hafnia. *J Cryst Growth* 2010;**312**:461–5.
17. Winter MR, Clarke DR. Thermal conductivity of yttria-stabilized zirconia–hafnia solid solutions. *Acta Mater* 2006;**54**:5051–9.
18. Wuchina E, Opila E, Opeka M, Fahrenholtz W, Talmy I. UHITCs: ultra-high temperature ceramic materials for extreme environment applications. *Electrochem Soc Interface* 2007;**16**:30–6.
19. Chen F, Huang L, Zhong Z, Gan GJ, Kwan SM, Kooli F. Synthesis of nanocrystalline tetragonal zirconia by inorganic metathesis reaction. *Mater Chem Phys* 2006;**97**:162–6.
20. Boskovic S, Djurovic D, Dohcevic-Mitrovic Z, Popovic Z, Zinkevich M, Aldinger F. Self-propagating room temperature synthesis of nanopowders for solid oxide fuel cells (SOFC). *J Power Sources* 2005;**145**: 237–42.
21. Chen W, Li F, Yu J. Combustion synthesis and characterization of nanocrystalline CeO_2-based powders via ethylene glycol–nitrate process. *Mater Lett* 2006;**60**:57–62.
22. Barraud E, Begin-Colin S, Le Caer G, Villieras F, Barres O. Thermal decomposition of $HfCl_4$ as a function of its hydration state. *J Solid State Chem* 2006;**179**:1842–51.
23. Physical constants of inorganic compounds.Lide DR, editor. *CRC handbook of chemistry and physics*. 78th ed. Boca Raton, FL: CRC Press; 1997. p. 4–60.
24. Hann RE, Suitch PR, Pentecost JL. Monoclinic crystal structure of ZrO_2 and HfO_2 refined from X-ray powder diffraction data. *J Am Ceram Soc* 1985;**68**:285–6.
25. Shannon RD. Revised effective ionic radii and systematic studies of interatomic distances in halides and chalcogenides. *Acta Crystallogr A* 1976;**32**:751–67.
26. Stefanic G, Music S. Thermal behavior of the amorphous precursors of the HfO_2–Fe_2O_3 system. *Thermochim Acta* 2001;**373**:59–67.
27. Toraya H, Yoshimura M, Somyja S. Analysis of the monoclinic-tetragonal ZrO_2 system by X-ray diffraction. *J Am Ceram Soc* 1984;**67**: 119–21.
28. Cullity BD, Stock SR. *Elements of X-ray diffraction*. 3rd ed. New Jersey: Prentice Hall; 2001.